

SUPPORTING INFORMATION

DESIGN NEW CARBAZOLE-BASED DYES FOR DYE-SENSITIZED SOLAR CELL: A LINEAR MODELS APPROACH

Emanuel F. dos S. Mattos^a, Carlos R. A. Daniel^b, Nivan B. da Costa Júnior^{a}*

^aDepartment of Chemistry, Federal University of Sergipe Foundation, Sergipe,
49100-000, Brazil

^bDepartment of Statistics, Federal University of Sergipe Foundation, Sergipe,
49100-000, Brazil

*Corresponding author. e-mail: nivan@academico.ufs.br

Trying to interpret the molecular descriptors

The interpretation of certain molecular descriptors – such as, for example, topological and electrotopological descriptors – can be a challenging task. In this context, for some best model's descriptors, we tried to establish correlations with chemically meaningful characteristics that are easier to interpret.

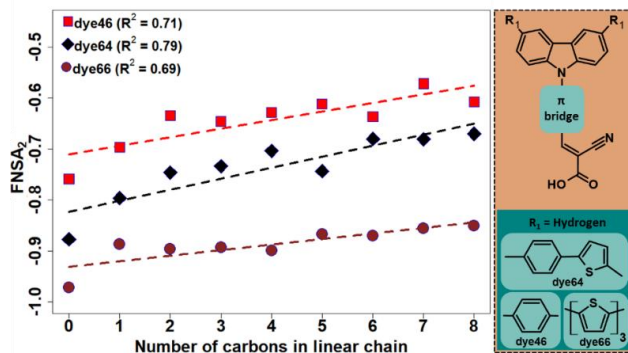
The descriptor $I_{434.46}$ is easily interpretable: dyes with strong absorptions in the 434 nm region tend to yield cells with higher PCEs. Thus, this descriptor reinforces the idea that sensitizers should absorb more intensely in the visible region to achieve higher PCEs^{1,2}. While it strengthens a well-known property of sensitizers, this descriptor does not indicate structural characteristics that are favorable for improving efficiency. However, some structural aspects are suggested by the descriptor $FNSA_2$ (Fractional Negative Surface Area), as given by Eq. 1 – for further details, see³.

$$FNSA_2 = \frac{Q^- \sum_a SA_a^-}{SASA} \quad (1)$$

Given that Q^- is the sum of all partial negative charges in the molecule, SA_a^- is the negative surface area on atom a accessible to the solvent, and $SASA$ corresponds to the solvent-accessible surface area. In this way, $FNSA_2$ indicates the fraction of the negatively charged molecule that the solvent can interact with. The structural information highlighted by this descriptor can be attributed to the effect of $SASA$. In other words, an increase in $SASA$ (Eq. 1) can reduce the absolute value of $FNSA_2$, which is associated with an increase in the predicted PCE. Then, some ways to increase the $SASA$ of the dye include, for example, elongating the π -bridge and/or introducing substitutions. In this regard, the literature reports the advantage of incorporating linear alkyl chains into sensitizers, as they reduce undesirable π - π interactions⁴.

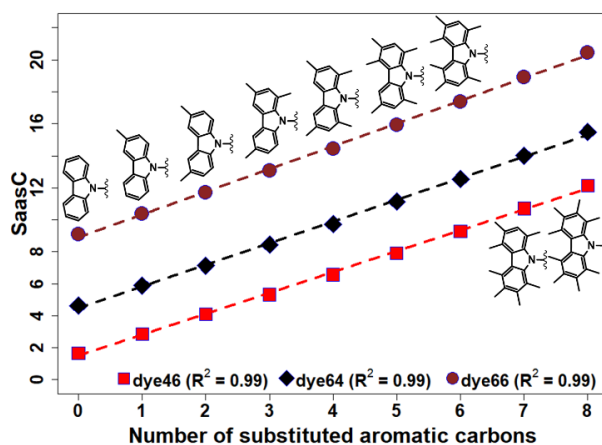
To observe the effect of altering the length of linear alkyl chains on the descriptor $FNSA_2$, we performed symmetrical substitutions on the donor group of three dyes (dye46, dye64, and dye66). In this way, it is possible to note the relationship between the increase in chain length and the descriptor $FNSA_2$ (Fig. 1), which supports the adoption of such chains for improving the efficiency of DSSCs⁴.

Figure 1. Influence of the length of linear alkyl chains on $FNSA_2$.



Moreover, the model provides an indication of positions that may have a negative effect on the predicted PCE if substitutions are made. This is given by $SaasC$, an electrotopological descriptor related to substituted aromatic carbons. More specifically, it is defined as the sum of the so-called E-State values of the substituted aromatic carbons – for further details, see ^{5,6}. In general, since $SaasC$ is always a positive value, an increase in the number of substituted aromatic positions leads to a decrease in the predicted PCE. In fact, when we successively increase the number of substituents, for example, on the donor group of the dye46, dye64, and dye66, a strong linear relationship between the two variables is observed (Fig. 2). That is, this descriptor appears to indicate a relationship between substituents at aromatic positions – and likely the characteristics of these substituents, since the *E-State* is influenced by the electronegativity of neighboring groups ^{5,6} – and the efficiency of the DSSC.

Figure 2. Variation of the $SaasC$ descriptor as a function of the number of methyl groups present in the donor group of the dye46, dye64, and dye66 structures.



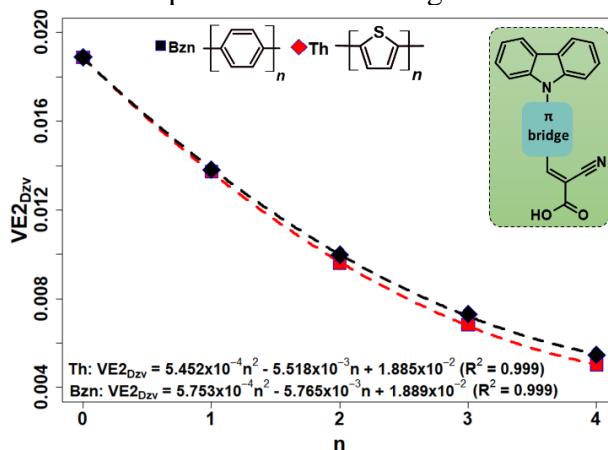
Two other electrotopological descriptors, minHBint8 and ndO , highlight the potential importance of electronegative species within the molecule and the modification of the dye's adsorption modes on the semiconductor surface, respectively. The

minHBint8 descriptor corresponds to the lowest E-state value among atoms that potentially form intramolecular hydrogen bonds at a distance of eight bonds. The influence of electronegativity arises from the tendency of E-state values to decrease when more electronegative species are present ⁵. On the other hand, ndO represents the number of oxygen atoms with double bonds present in the molecule, which could result in an adsorption mode that reduces electron injection into the semiconductor's conduction band.

The autocorrelation descriptors (*ATS6m*, *ATSC6i*, *AATSC5s*, *MATS4s*, and *GATS7c*) indicate how a specific property (electronegativity, charge, mass, volume, etc.) is distributed across a molecule with N atoms ⁷. In general, these descriptors highlight the importance of: 1) an increase in the mass/volume of the dye, which tends to elevate the predicted PCE, supporting the increase in solvent-accessible area; and 2) the presence of atoms with higher ionization energies or more electronegative characteristics.

Finally, the M-3 model presents four descriptors obtained through the eigenvalues of certain matrices ($VE2_{Dzv}$, $VE3_{Dt}$, $SpMin1_{Bhi}$, and $BCUTc_{1l}$) ⁸. Of this set, $VE2_{Dzv}$ is given by the average of the coefficients of the last eigenvector of the Barysz matrix weighted by van der Waals (vdW) volumes and shows a strong correlation with, for example, the number of rings present in the π -bridge (Fig. 3). In other words, $VE2_{Dzv}$ indicates that an increase in the π -bridge tends to elevate the PCE of the cell. On the other hand, $VE3_{Dt}$ – obtained by summing the coefficients of the last eigenvector of the detour matrix – shows identical values for similar structures, such as dye39 and dye40 (9.34), but experiences considerable variations when there is an increase in molecular branching, as seen with dye29 (-12.54), dye30 (-6.21), and dye87 (-6.38) and dye88 (-2.77).

Figure 3. Variation of the $VE2_{Dzv}$ descriptor as a function of the number of rings present in the π -bridge.



The $SpMin1_{Bhi}$ is obtained from the absolute value of the smallest eigenvalue of the Burden matrix weighted by the first ionization potential. Due to the property used in the weighting, it is expected that changes in the value of $SpMin1_{Bhi}$ are associated with the ionization potential of the molecule ⁷. Finally, $BCUTc_{1l}$ – which corresponds to the first smallest eigenvalue of the Burden matrix weighted by partial charges – reinforces the idea presented by the set of autocorrelation descriptors.

De modo geral, o modelo M-3 apresenta um poder de predição similar aos modelos propostos por Krishnaa *et al.*⁹ e, a partir da análise dos descritores realizada acima, também é possível notar certas semelhanças entre as características estruturais indicadas pelos modelos como, por exemplo, a presença de cadeias alquílicas para a redução de interações π - π . Todavia, o M-3 apresenta características não indicadas pelos modelos de Krishnaa, tais como: absorção na região do visível, substituição de carbonos aromáticos e comprimento da ponte π . Em suma, o nosso melhor modelo fornece um complemento de informações acerca de importantes características estruturais para um sensibilizador baseado carbazol atuar suficientemente bem em uma DSSC.

In general, the M-3 model demonstrates predictive power similar to the models proposed in the literature ⁹, and from the analysis of the descriptors presented above, it is also possible to observe certain similarities between the structural features indicated by the models, such as the presence of alkyl chains to reduce π - π interactions. However, the M-3 model introduces some new characteristics that were not previously indicated, such as absorption in the visible region, substitution of aromatic carbons, and the length of the π -bridge. In summary, our best model provides complementary information regarding important structural features for a carbazole-based sensitizer to perform adequately in a DSSC.

References

- (1) Grätzel, M. Solar Energy Conversion by Dye-Sensitized Photovoltaic Cells. *Inorganic Chemistry*. October 3, 2005, pp 6841–6851. <https://doi.org/10.1021/ic0508371>.
- (2) Arkan, F.; Izadyar, M. Recent Theoretical Progress in the Organic/Metal-Organic Sensitizers as the Free Dyes, Dye/TiO₂ and Dye/Electrolyte Systems; Structural Modifications and Solvent Effects on Their Performance. *Renewable and Sustainable Energy Reviews*. Elsevier Ltd October 1, 2018, pp 609–655. <https://doi.org/10.1016/j.rser.2018.06.054>.

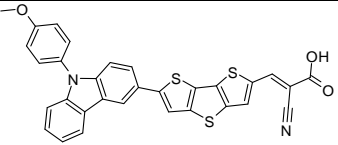
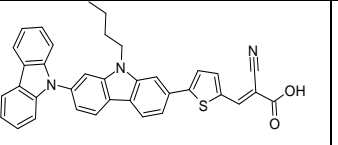
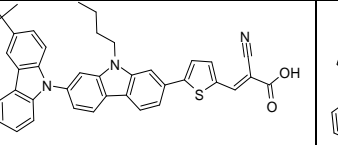
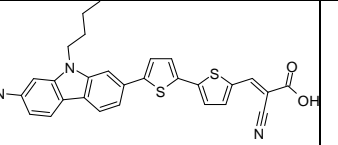
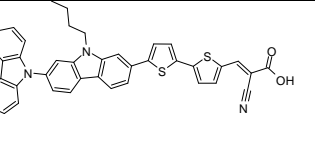
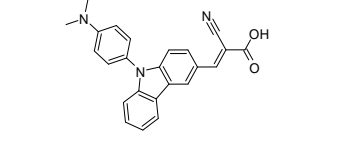
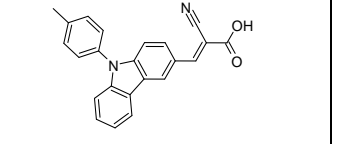
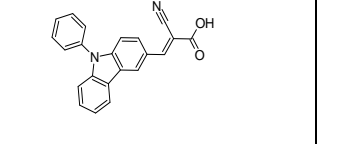
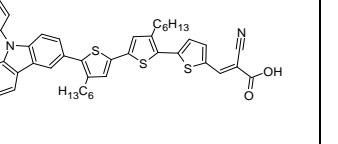
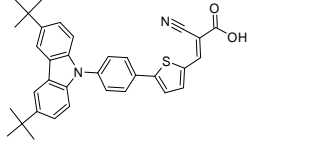
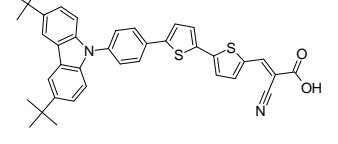
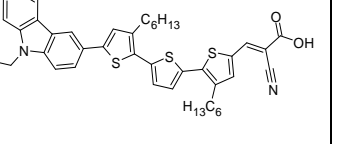
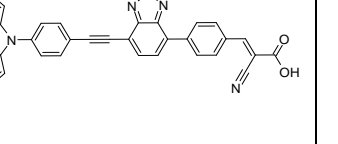
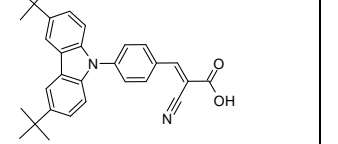
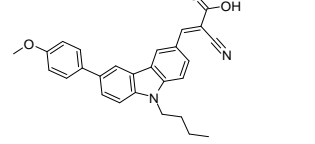
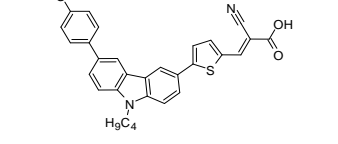
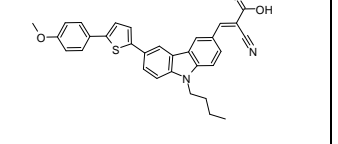
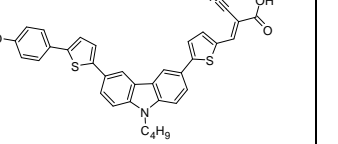
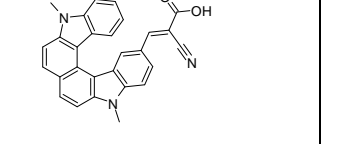
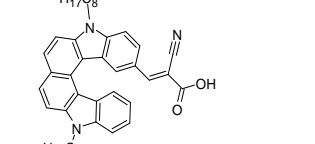
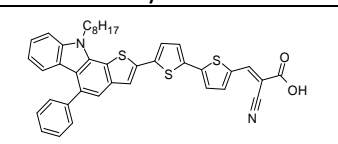
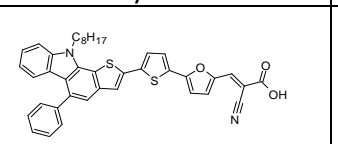
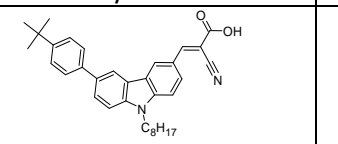
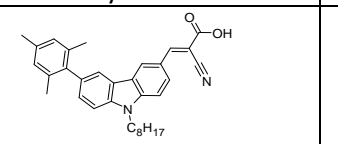
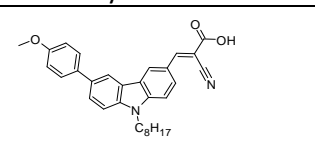
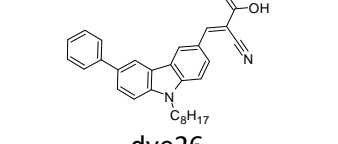
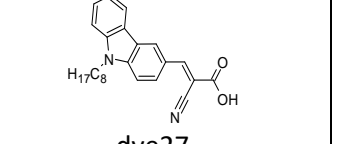
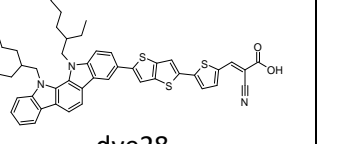
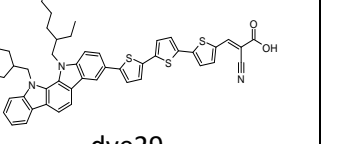
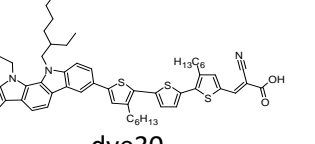
- (3) Stanton, D. T.; Jurs, P. C. Development and Use of Charged Partial Surface Area Structural Descriptors in Computer-Assisted Quantitative Structure-Property Relationship Studies. *Anal Chem* **1990**, *62* (21), 2323–2329. https://doi.org/10.1021/AC00220A013/ASSET/AC00220A013.FP.PNG_V03.
- (4) Ezhumalai, Y.; Lee, B.; Fan, M. S.; Harutyunyan, B.; Prabakaran, K.; Lee, C. P.; Chang, S. H.; Ni, J. S.; Vegiraju, S.; Priyanka, P.; Wu, Y. W.; Liu, C. W.; Yau, S.; Lin, J. T.; Wu, C. G.; Bedzyk, M. J.; Chang, R. P. H.; Chen, M. C.; Ho, K. C.; Marks, T. J. Metal-Free Branched Alkyl Tetrathienoacene (TTAR)-Based Sensitizers for High-Performance Dye-Sensitized Solar Cells. *J Mater Chem A Mater* **2017**, *5* (24), 12310–12321. <https://doi.org/10.1039/c7ta01825h>.
- (5) Hall, L. H.; Kier, L. B. Electrotological State Indices for Atom Types: A Novel Combination of Electronic, Topological, and Valence State Information. *J Chem Inf Comput Sci* **1995**, *35* (6), 1039–1045. https://doi.org/10.1021/CI00028A014/ASSET/CI00028A014.FP.PNG_V03.
- (6) Hall, L. H.; Mohny, B.; Kier, L. B. The Electrotological State: Structure Information at the Atomic Level for Molecular Graphs. *J Chem Inf Comput Sci* **1991**, *31* (1), 76–82. https://doi.org/10.1021/CI00001A012/ASSET/CI00001A012.FP.PNG_V03.
- (7) Todeschini, R.; Consonni, V. Molecular Descriptors for Chemoinformatics: Volume I: Alphabetical Listing / Volume II: Appendices, References, Volume 41. *Prevention* **2009**, 27–31.
- (8) Todeschini, R.; Consonni, V. *Molecular Descriptors for Chemoinformatics, Volumes I & II*; 2009.
- (9) Krishna, J. G.; Ojha, P. K.; Kar, S.; Roy, K.; Leszczynski, J. Chemometric Modeling of Power Conversion Efficiency of Organic Dyes in Dye Sensitized Solar Cells for the Future Renewable Energy. *Nano Energy* **2020**, *70*. <https://doi.org/10.1016/j.nanoen.2020.104537>.

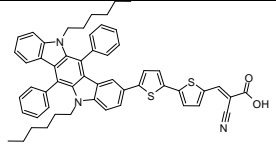
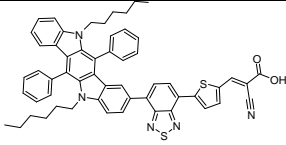
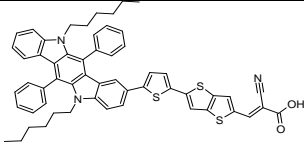
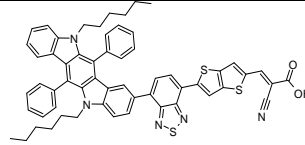
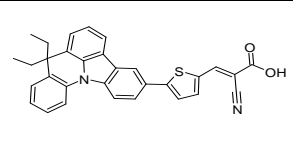
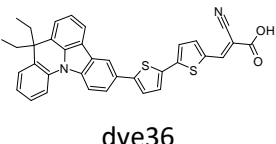
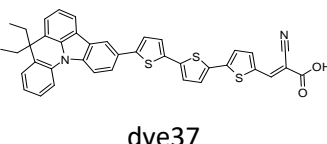
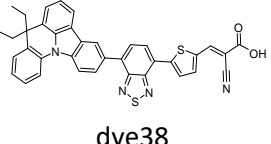
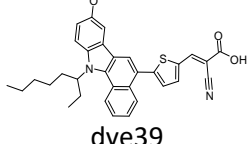
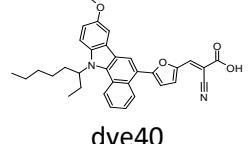
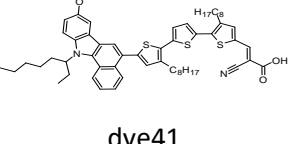
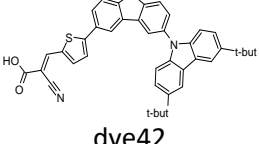
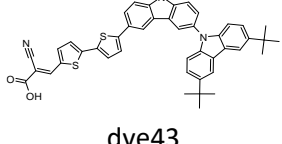
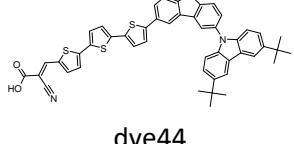
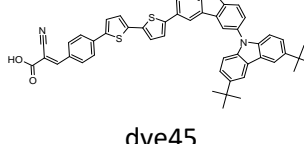
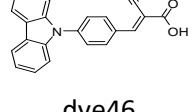
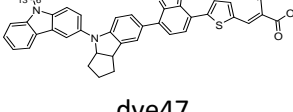
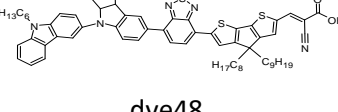
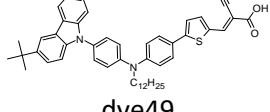
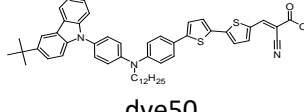
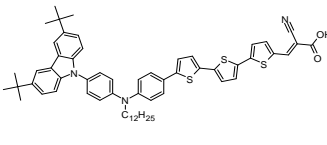
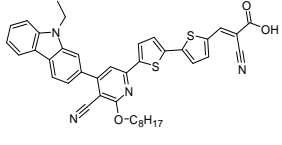
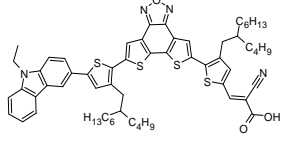
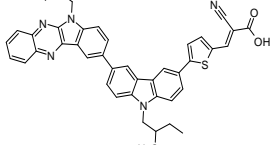
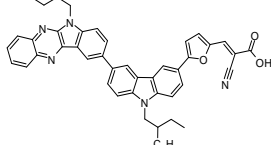
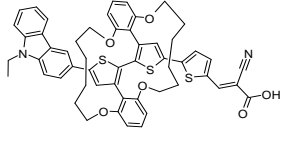
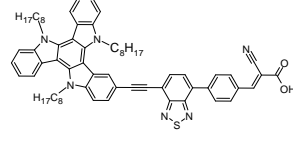
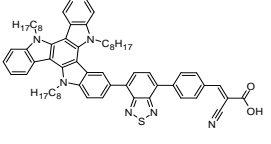
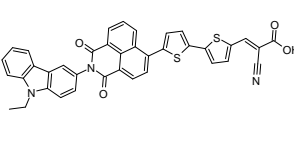
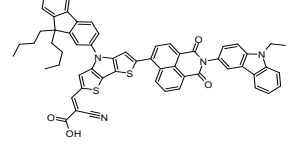
Table S1. Dye Structures and Photovoltaic Performances

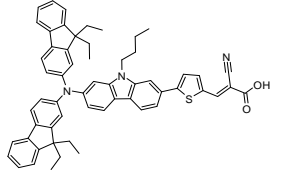
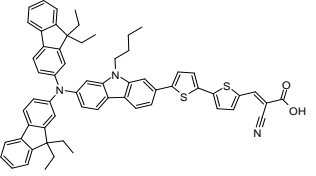
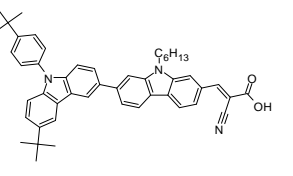
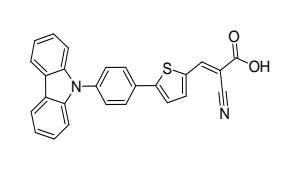
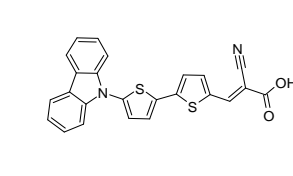
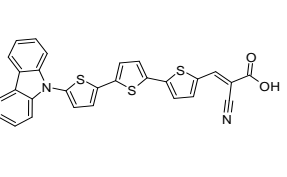
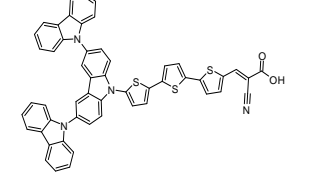
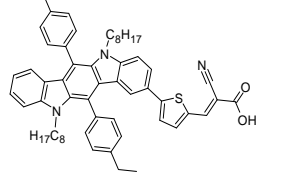
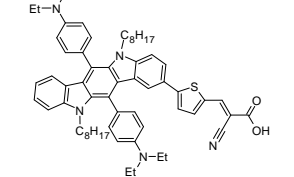
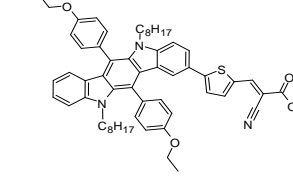
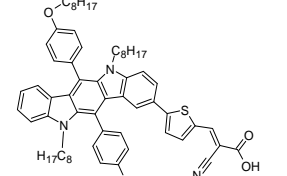
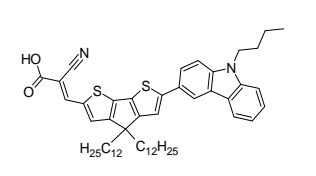
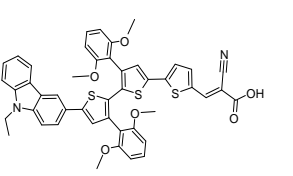
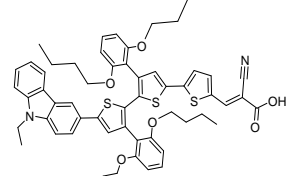
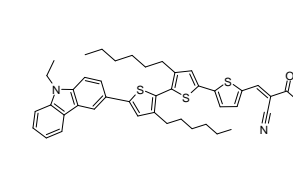
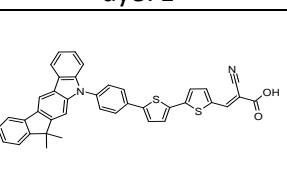
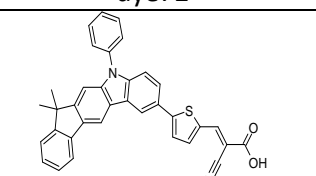
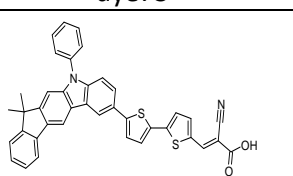
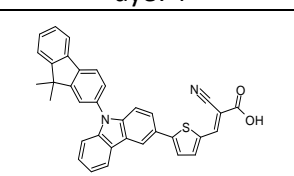
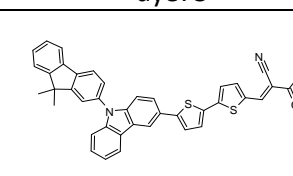
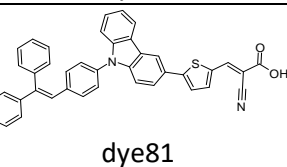
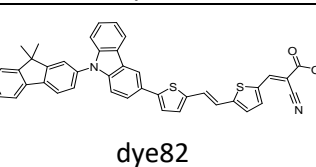
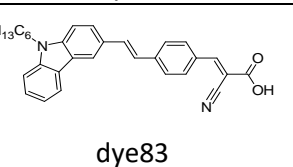
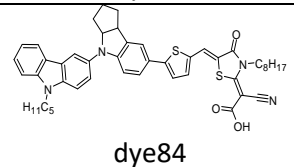
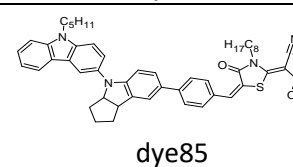
Dye	%PCE	Sol.	doi	Dye	%PCE	Sol.	doi
1.	5.64	Et	10.1016/j.tet.2013.02.058	33.	4.11	THF	10.1039/C3TA11748K
2.	4.22	Di	10.1021/am404948w	34.	6.40	THF	10.1039/C3TA11748K
3.	4.95	Di	10.1021/am404948w	35.	5.43	THF	10.1039/C3TA01657A
4.	6.04	Di	10.1021/am404948w	36.	6.50	THF	10.1039/C3TA01657A
5.	5.48	Di	10.1021/am404948w	37.	2.96	THF	10.1039/C3TA01657A
6.	1.21	Ac	10.1108/PRT-09-2014-0077	38.	4.61	THF	10.1039/C3TA01657A
7.	2.82	Ac	10.1108/PRT-09-2014-0077	39.	6.01	Di	10.1021/am508400a
8.	3.69	Ac	10.1108/PRT-09-2014-0077	40.	6.93	Di	10.1021/am508400a
9.	5.92	Ac	10.1016/j.jpowsour.2020.227776	41.	7.54	Di	10.1021/am508400a
10.	2.39	Tr	doi.org/10.1021/jp1055842	42.	3.64	Di	10.1002/ejoc.201300373
11.	2.48	Tr	doi.org/10.1021/jp1055842	43.	4.80	Di	10.1002/ejoc.201300373
12.	7.44	Tr	10.1016/j.electacta.2018.08.068	44.	5.69	Di	10.1002/ejoc.201300373
13.	3.50	Tr	10.1016/j.dyepig.2016.08.013	45.	4.62	Di	10.1002/ejoc.201300373
14.	2.68	Ac	10.1246/cl.2010.864	46.	1.77	Di	10.1016/j.dyepig.2012.03.028
15.	1.87	Di	10.1002/ejoc.201600353	47.	5.13	Di	10.1021/acsami.5b08888
16.	4.54	Di	10.1002/ejoc.201600353	48.	7.69	Di	10.1021/acsami.5b08888
17.	2.52	Di	10.1002/ejoc.201600353	49.	3.52	Di	10.1021/jp304489t
18.	4.57	Di	10.1002/ejoc.201600353	50.	4.10	Di	10.1021/jp304489t
19.	2.49	Tr	10.1016/j.solmat.2009.11.014	51.	5.12	Di	10.1021/jp304489t
20.	3.18	Tr	10.1016/j.solmat.2009.11.014	52.	3.34	Di	10.1016/j.solener.2018.09.073
21.	6.60	Tr	10.1016/j.tet.2014.01.001	53.	5.98	THF	10.1021/am5067145
22.	6.73	Tr	10.1016/j.tet.2014.01.001	54.	6.48	Di	10.1016/j.jpowsour.2015.01.148
23.	2.17	Tr	10.1039/C6RA01185C	55.	7.03	Di	10.1016/j.jpowsour.2015.01.148
24.	0.98	Tr	10.1039/C6RA01185C	56.	9.20	Di	10.1039/C3TA12368E
25.	2.69	Tr	10.1039/C6RA01185C	57.	7.15	Di	10.1039/C7NJ04629D
26.	0.98	Tr	10.1039/C6RA01185C	58.	7.26	Di	10.1039/C7NJ04629D
27.	1.11	Tr	10.1039/C6RA01185C	59.	0.57	Di	10.1007/s10854-018-9750-4
28.	5.78	Tr	10.1016/j.dyepig.2019.01.033	60.	0.92	Di	10.1007/s10854-018-9750-4
29.	5.23	Tr	10.1016/j.dyepig.2019.01.033	61.	6.44	Di	10.1016/j.dyepig.2015.07.034
30.	5.97	Tr	10.1016/j.dyepig.2019.01.033	62.	4.77	Di	10.1016/j.dyepig.2015.07.034
31.	6.09	THF	10.1039/C3TA11748K	63.	4.38	Di	10.1016/j.dyepig.2015.09.004
32.	5.55	THF	10.1039/C3TA11748K	64.	2.74	Di	10.1016/j.dyepig.2013.09.025

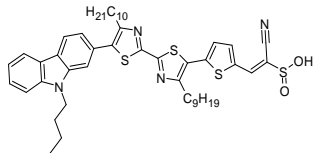
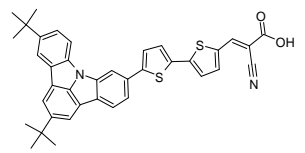
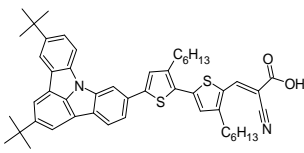
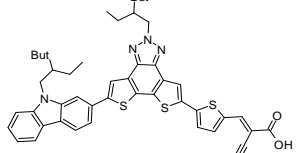
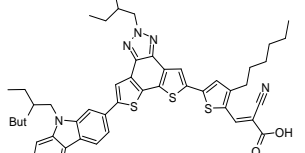
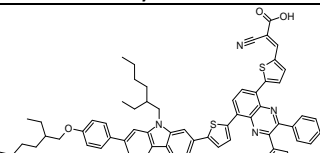
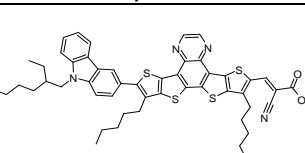
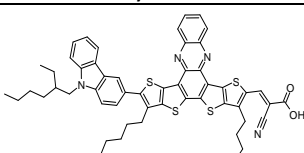
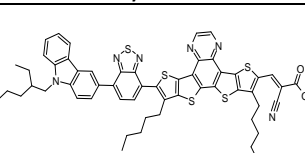
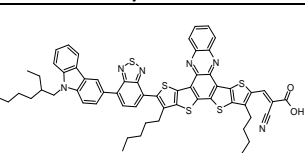
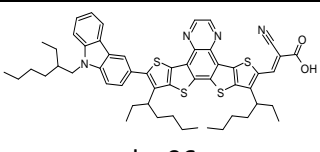
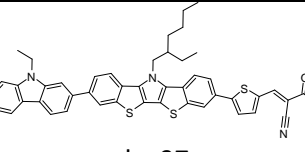
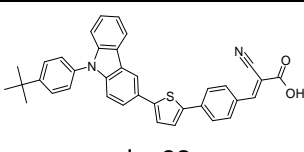
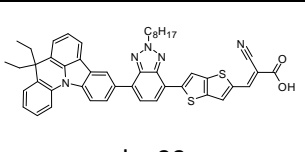
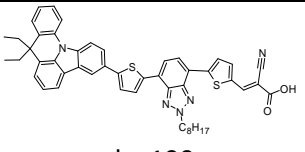
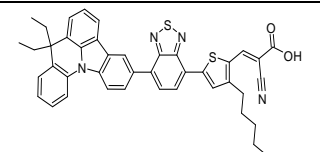
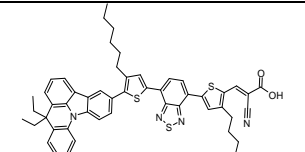
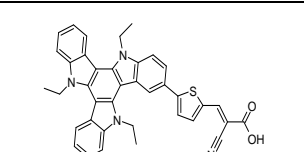
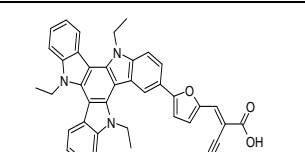
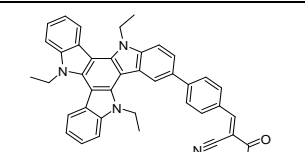
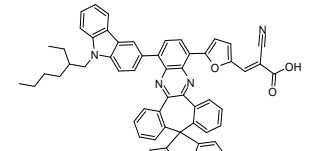
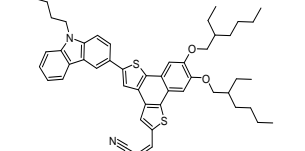
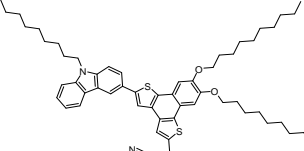
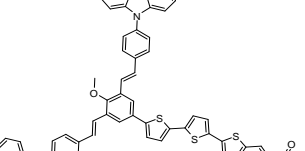
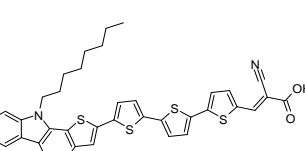
65.	2.94	Di	10.1016/j.dyepig.2013.09.025	96.	5.23	THF	10.1016/j.dyepig.2018.06.010
66.	4.30	Di	10.1016/j.dyepig.2013.09.025	97.	5.30	THF	10.1016/j.dyepig.2018.10.004
67.	4.86	Di	10.1016/j.dyepig.2013.09.025	98.	5.65	THF	10.1039/C3RA43057J
68.	6.25	Di	10.1016/j.jpowsour.2016.04.043	99.	6.23	THF	10.1039/C3RA43057J
69.	8.09	Di	10.1016/j.jpowsour.2016.04.043	100.	7.15	THF	10.1039/C3RA43057J
70.	6.98	Di	10.1016/j.jpowsour.2016.04.043	101.	5.20	THF	10.1039/C3RA43057J
71.	7.58	Di	10.1016/j.jpowsour.2016.04.043	102.	5.82	THF	10.1039/C3RA43057J
72.	7.50	Di	10.1039/C3RA22249G	103.	6.10	THF	10.1021/ol402931u
73.	7.01	Di	10.1039/C9TC01520E	104.	5.50	THF	10.1021/ol402931u
74.	8.01	Di	10.1039/C9TC01520E	105.	5.11	THF	10.1021/ol402931u
75.	5.06	Di	10.1039/C9TC01520E	106.	4.87	Di	10.1002/gch2.201900034
76.	4.23	DMF	10.1039/C7PP00350A	107.	4.49	THF	10.1039/C3TA12901B
77.	5.97	DMF	10.1039/C7PP00350A	108.	4.60	THF	10.1039/C3TA12901B
78.	5.34	DMF	10.1039/C7PP00350A	109.	3.03	THF	10.1002/asia.201402654
79.	5.02	Et	10.1016/j.tet.2006.12.082	110.	5.9	Tr	10.1039/C4QO00285G
80.	5.15	Et	10.1016/j.tet.2006.12.082	111.	6.5	Tr	10.1039/C4QO00285G
81.	3.87	Et	10.1016/j.tet.2006.12.082	112.	7.0	Tr	10.1039/C4QO00285G
82.	3.76	Et	10.1016/j.tet.2006.12.082	113.	4.31	Et	10.1021/jp906334w
83.	7.1	Et	10.1039/C5TA06548H	114.	5.96	Tr	10.1016/j.tet.2015.04.018
84.	8.48	Met	10.1016/j.dyepig.2018.03.072	115.	5.2	Di	10.1016/j.dyepig.2015.02.020
85.	4.69	Met	10.1016/j.dyepig.2018.03.072	116.	6.5	Di	10.1016/j.dyepig.2015.02.020
86.	4.65	THF	10.1016/j.dyepig.2012.10.002	117.	6.5	Di	10.1016/j.dyepig.2015.02.020
87.	3.96	THF	10.1039/C5RA02720A	118.	6.95	Di	10.1039/C4TA05162A
88.	2.85	THF	10.1039/C5RA02720A	119.	6.67	Di	10.1039/C4TA05162A
89.	7.52	THF	10.1039/C6TA02275H	120.	2.30	Di	10.1021/jo200501b
90.	8.51	THF	10.1039/C6TA02275H	121.	3.19	Di	10.1016/j.tetlet.2014.04.037
91.	7.58	THF	10.1016/j.dyepig.2016.12.013	122.	5.10	Di	10.1021/am500947k
92.	6.48	THF	10.1016/j.dyepig.2018.06.010	123.	4.90	Di	10.1002/cssc.201200975
93.	6.33	THF	10.1016/j.dyepig.2018.06.010	124.	5.80	Di	10.1002/cssc.201200975
94.	7.77	THF	10.1016/j.dyepig.2018.06.010	125.	5.80	Di	10.1002/cssc.201200975
95.	5.23	THF	10.1016/j.dyepig.2018.06.010	126.	5.60	Di	10.1002/cssc.201200975

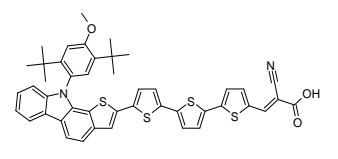
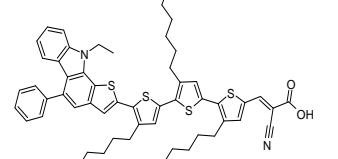
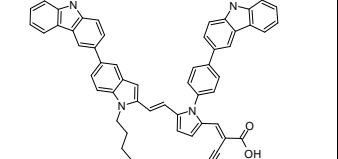
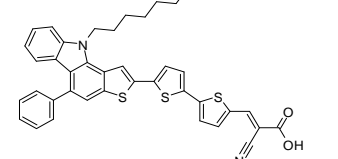
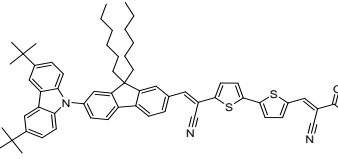
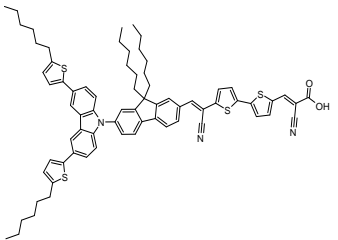
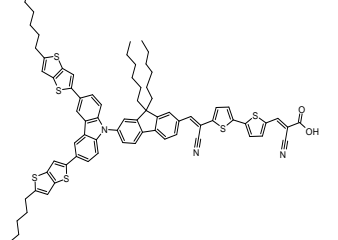
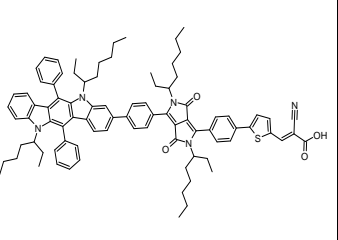
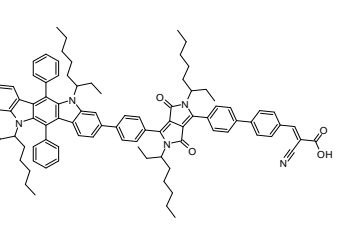
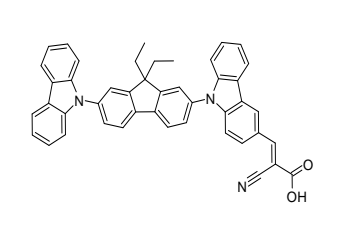
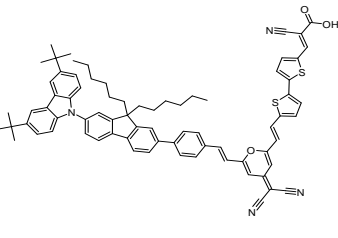
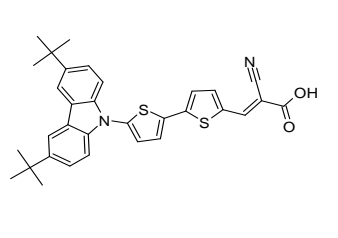
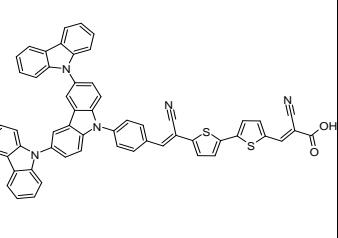
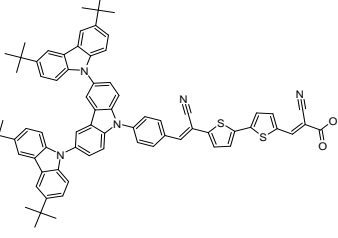
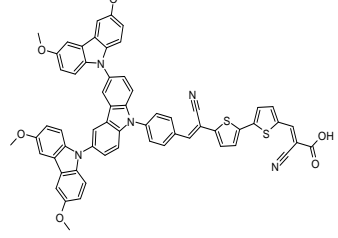
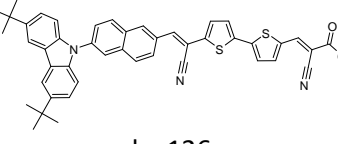
Ac – Acetonitrile; **Et** – Ethanol; **Di** – Dichloromethane; **DMF** - Dimethylformamide; **Met** – Methanol; **Tr** – Trichloromethane; **THF** – Tetrahydrofuran;

				
dye31	dye32	dye33	dye34	dye35
				
dye36	dye37	dye38	dye39	dye40
				
dye41	dye42	dye43	dye44	dye45
				
dye46	dye47	dye48	dye49	dye50
				
dye51	dye52	dye53	dye54	dye55
				
dye56	dye57	dye58	dye59	dye60

				
dye61	dye62	dye63	dye64	dye65
				
dye66	dye67	dye68	dye69	dye70
				
dye71	dye72	dye73	dye74	dye75
				
dye76	dye77	dye78	dye79	dye80
				
dye81	dye82	dye83	dye84	dye85

				
dye86	dye87	dye88	dye89	dye90
				
dye91	dye92	dye93	dye94	dye95
				
dye96	dye97	dye98	dye99	dye100
				
dye101	dye102	dye103	dye104	dye105
				
dye106	dye107	dye108	dye109	dye110

 <p>dye111</p>	 <p>dye112</p>	 <p>dye113</p>	 <p>dye114</p>	 <p>dye115</p>
 <p>dye116</p>	 <p>dye117</p>	 <p>dye118</p>	 <p>dye119</p>	 <p>dye120</p>
 <p>dye121</p>	 <p>dye122</p>	 <p>dye123</p>	 <p>dye124</p>	 <p>dye125</p>
 <p>dye126</p>				